

Barrier-Controlled Non-Equilibrium Criticality in Reactive Particle Systems

Qun-Li Lei^a, Hao Hu^b, and Ran Ni^{a,1}

^aSchool of Chemical and Biomedical Engineering, Nanyang Technological University, 62 Nanyang Drive, 637459, Singapore; ^bSchool of Physics and Materials Science, Anhui University, Hefei 230601, China

This manuscript was compiled on March 27, 2025

Non-equilibrium critical phenomena generally exist in many dynamic systems, like chemical reactions, epidemic spreading and some driven-dissipative particle systems. Here, by using computer simulation and theoretical analysis, we demonstrate the crucial role of the activation barrier on the criticality of non-equilibrium phase transitions using a minimal reactive hard-sphere model. We find that at zero thermal noise, with increasing the activation barrier, the type of transition changes from a continuous conserved directed percolation into a discontinuous dynamic transition by crossing a tricritical point. A mean-field theory is proposed to explain this phenomenon, which suggests that the transition at finite thermal noise belongs to the Ising universality. Moreover, we obtain the tricritical exponents in the system which quantitatively agree with field theory simulations.

Non-equilibrium critical phenomena | reaction barrier | tricritical point | directed percolation | Ising universality

Non-equilibrium critical phenomena (1, 2) generically exist in various systems, e.g., chemical reactions (3, 4), epidemic spreads (5), brain activities (6), colloidal and granular systems (7–10), turbulence and active fluids (11–14) etc. At the critical point, these systems exhibit scaling-invariance accompanied by diverging correlation lengths and time scales, which can be characterized by some generic critical exponents (2). The directed percolation (DP) exemplified by the lattice contact model (15) is among the best-known universality classes of non-equilibrium phase transitions, yet deviation from the DP universality is also found in many dynamic systems (2). For examples, by introducing particle number conservation, a new universality of conserved direction percolation (CDP) was found in the Manna model (16) and conserved lattice gas model (17), while in the Schlogl's second model aiming to model the cooperative surface catalytic reaction, the dynamic transition becomes first-order (3). However, these lattice models fail in revealing the physics of non-equilibrium criticality in many real dynamic systems, e.g., chemical reactions, in which the kinetic energy, particle inertia, momentum conservation and some barrier-crossing processes play important roles. Thus, it remains unclear whether there is any overlooked but fundamental mechanism controlling the non-equilibrium criticality in those real dynamic systems.

To this end, here we investigate a minimal reactive hard sphere model with an activation barrier, which captures the essential physics of many non-equilibrium particle systems. For examples, this model can be regarded as a simplified version of the Semenov hard sphere model for exothermic chemical reactions (18–21). The Semenov model, which assumes a uniform temperature distribution and neglects the reactant consumption at ignition, is the first theory of thermal explosion (22, 23). The model can also be viewed as a modification of random-organization hard sphere model with the

addition of an activation barrier. The random-organization was originally proposed to model colloidal particle system under oscillatory shearing (7, 8, 24–26), while it exhibits generic non-equilibrium phase transitions, which also have connections with the yielding of amorphous solids (9, 27), the jamming transition (28–33), memory formation (34), depinning transition of driven vortices (35–37), dynamic hyperuniform states (38–45) etc. By using simulation and theory, we prove that the activation barrier controls the criticality or “sharpness” of the no-equilibrium phase transition in the system: at zero thermal noise, increasing the activation barrier changes the type of absorbing transition from a continuous CDP to a discontinuous dynamic transition by crossing a *tricritical* point, while at finite thermal noise, the transition becomes the Ising-type.

Result

Model and Simulation. The model we consider consists of N hard spheres with the same mass m and diameter σ . Activations occur in pairwise collisions between two particles, if their relative kinetic energy along the center-to-center direction surpasses the activation barrier E_b . During each activation, an energy ϵ is released in the center-to-center direction, with the momentum of the two particles conserved. The motion of particles obeys the Langevin dynamics between two consecutive collisions. For particle i , the equation of motion can be

Significance Statement

Non-equilibrium critical phenomena are usually studied in lattice models, like the classical contact model for epidemic spreads. However, these lattice models fail in revealing the physics of non-equilibrium criticality in many real dynamic systems, e.g., chemical reactions, in which the kinetic energy, particle inertia, momentum conservation and some barrier-crossing processes play important roles. Here we study a minimal reactive hard-sphere model with an activation barrier that captures the essential physics of exothermic chemical reactions and some random-organization processes. We prove that activation barrier controls the criticality or “sharpness” of the non-equilibrium phase transitions, which also shed light on the understanding of the critical behaviour of amorphous materials, active matter, and the spread of epidemic, knowledge and innovations.

Author contributions: Q.-L.L. and R.N. designed the research; Q.-L.L. performed research; all authors discussed the results and wrote the manuscript.

The authors declare no conflict of interest.

¹To whom correspondence should be addressed. E-mail: r.ni@ntu.edu.sg

written as

$$m \frac{d\mathbf{v}_i(t)}{dt} = -\gamma \mathbf{v}_i(t) + \sqrt{2\gamma k_B T} \eta(t), \quad [1]$$

where γ is the damping coefficient. The second noise term is based on the fluctuation-dissipation theorem with T the thermal temperature and $\eta(t)$ the Gaussian white noise. This model is a direct generalization of the random-organizing hard-sphere model with the addition of an activation barrier and thermal noise (44). It can also be seen as a simplified version of the Semenov reactive hard-sphere model for exothermic chemical reactions, in which non-consumable reactants are confined by two parallel slabs which are connected with thermal reservoir at a fixed temperature (18–21). Here, in our model the boundary thermalization is treated implicitly through a Langevin thermostat.

The dimensionality of the system we study is $d = 2, 3$ with periodic boundary conditions in all directions. The reduced particle density of the system is defined as $\tilde{\rho} = N\sigma^d/V$ with $V = L^d$ the volume of the system and L the box length. We adopt an event-driven algorithm (44, 46) to simulate the system in both 2D and 3D. The typical excitation speed is defined as $v_0 = \sqrt{\epsilon/m}$, and the time unit of the system is set as $\tau_0 = \sigma/v_0$. The typical dissipation time is $\tau_d = m/\gamma$.

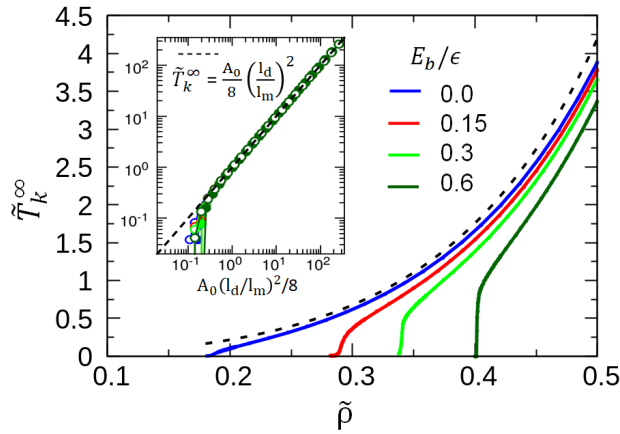


Fig. 1. Barrier-controlled transition sharpness. \tilde{T}_k^∞ as a function of density for 2D system with different E_b . Inset: \tilde{T}_k^∞ as a function of l_d ($\tilde{\rho} = 0.1$) and l_m ($l_d = 160\sigma$). The dashed lines are the theoretical predictions with $A_0 = 1.56$.

Critical phenomena. We first study the 2D system at $T = 0$. In this case, as shown in Ref (44), there are two important characteristic lengths in the system, i.e., the mean free path l_m and the dissipation length $l_d = \sqrt{m\epsilon}/\gamma$, i.e., the typical distance that an isolated particle can travel after being activated by collision. The later is the typical distance that isolated particles can travel after a single activation. With increasing the ratio l_d/l_m , the system undergoes a dynamic absorbing-active phase transition at $l_d \simeq l_m$ (44). Here, the absorbing state corresponds to the zero kinetic energy state while the active state has a positive kinetic temperature. Thus, the reduced kinetic temperature of the system can be chosen as the order parameter of the system, i.e.,

$$\tilde{T}_k(t) = \frac{dk_B T_k(t)}{\epsilon} \quad \text{and} \quad k_B T_k(t) = \frac{m \langle v^2(t) \rangle}{d}. \quad [2]$$

Here, $\overline{v^2}$ is the average square of speed of all particles and $\langle \cdot \rangle$ calculates the ensemble average of active (surviving) trials (17).

In Fig. 1, we plot \tilde{T}_k as a function of density for systems with different activation barriers. With increasing E_b , the transition shifts to the higher density regime and becomes sharper, similar to the explosive percolation (47). To determine the type of the transitions, we assume there is a scaling-invariant critical point $\tilde{\rho}_c$ in the system and perform finite-size analysis to determine $\tilde{\rho}_c$ and the corresponding critical exponents. For systems near the critical point, the saturated kinetic temperature $\tilde{T}_k^\infty(\Delta\tilde{\rho}, L)$ satisfies the scaling relationship (2, 17),

$$\tilde{T}_k^\infty(\Delta\tilde{\rho}, L) = L^{-\beta/\nu_\perp^*} \mathcal{G}\left(L^{1/\nu_\perp^*} \Delta\tilde{\rho}\right), \quad [3]$$

where $\Delta\tilde{\rho} = \tilde{\rho} - \tilde{\rho}_c$ and $\mathcal{G}(\cdot)$ is the scaling function. For systems at the critical point ($\Delta\tilde{\rho} = 0$), starting from random initial configurations, $\tilde{T}_k(t)$ follows a power-law decay $t^{-\alpha}$ before reaching the saturated value satisfying $\tilde{T}_k^\infty \sim L^{-\beta/\nu_\perp^*}$. In Fig. 2A, we show the decay of $\tilde{T}_k(t)$ for a 2D system of different size $L \propto N^{1/d}$ for $E_b = 0$ and $l_d = 2\sigma$. The inset plots \tilde{T}_k^∞ as a function of L . Both figures indicate the scaling-invariance and we obtain the corresponding critical exponents $\alpha = 0.54$ and $\beta/\nu_\perp^* = -0.77$. In Fig. 2D, we plot the collapse of $\tilde{T}_k^\infty(\Delta\tilde{\rho}, L)$ for different L (solid symbols) based on Eq. (3) with $\beta = 0.64$ and $\nu_\perp^* = 0.84$, which is consistent with the obtained β/ν_\perp^* . We also use another finite-size scaling method to obtain $z = 1.50$ (See Section A and Fig. S1 in *SI Appendix* for details). These exponents for $E_b = 0$ are summarized in Table I, which indicates that the universality of this phase transition belongs to CDP or Manna class (16, 44). Nevertheless, with a similar analysis for systems of $E_b = 0.165\epsilon$ in Fig. 2B,D, and Fig. S2 in *SI Appendix*, we obtain critical exponents distinct from CDP (Table I). As shown later, these unreported exponents appear because the system is at a *tricritical* point, which separates the continuous and discontinuous transitions. Indeed, by further increasing E_b to 0.3ϵ , we find the finite-size scaling breaks down and the system exhibits the bistability at $k_B T = 0.02\epsilon$ (Fig. 2C). In Fig. 2F, we further show the appearance of cusp bifurcation and hysteresis loop with increasing the activation barrier at finite temperature. Therefore, the system undergoes a discontinuous transition at large activation barrier even with a finite thermal noise.

To determine the tricritical point, we employ a crossover scaling analysis (48–50). Supposing $E_{b,c}$ is the tricritical energy barrier and letting $\Delta E_b = E_b - E_{b,c}$, the crossover scaling can be written as

$$\tilde{T}_k(\Delta\tilde{\rho}, \Delta E_b) = \Delta E_b^{-\beta_t/\phi} \mathcal{G}_t(\Delta\tilde{\rho} \Delta E_b^{-1/\phi}), \quad [4]$$

given $\Delta\tilde{\rho} \ll \Delta E_b/\epsilon$ (48). Here, the scaling function $\mathcal{G}_t(x) \sim x^\beta$ when $x \ll 1$ and $\mathcal{G}_t(x) \sim x^{\beta_t}$ when $x \gg 1$ with β_t the tricritical exponent. In Fig. 2E, we show the collapse of $\tilde{T}_k(\Delta\tilde{\rho})$ for systems with different E_b (solid symbols), which leads to $E_{b,c} = 0.165\epsilon$ and $\phi = 0.32$.

Mean-field theory. In the following, we formulate an analytical theory to explain the above complex phase behaviors. At the mean-field level, generally the activation driving power W_{driv} and the dissipation power W_{disp} per particle are (44)

$$W_{driv} = f_a \epsilon, \quad W_{disp} = \overline{v^2} \gamma \quad [5]$$

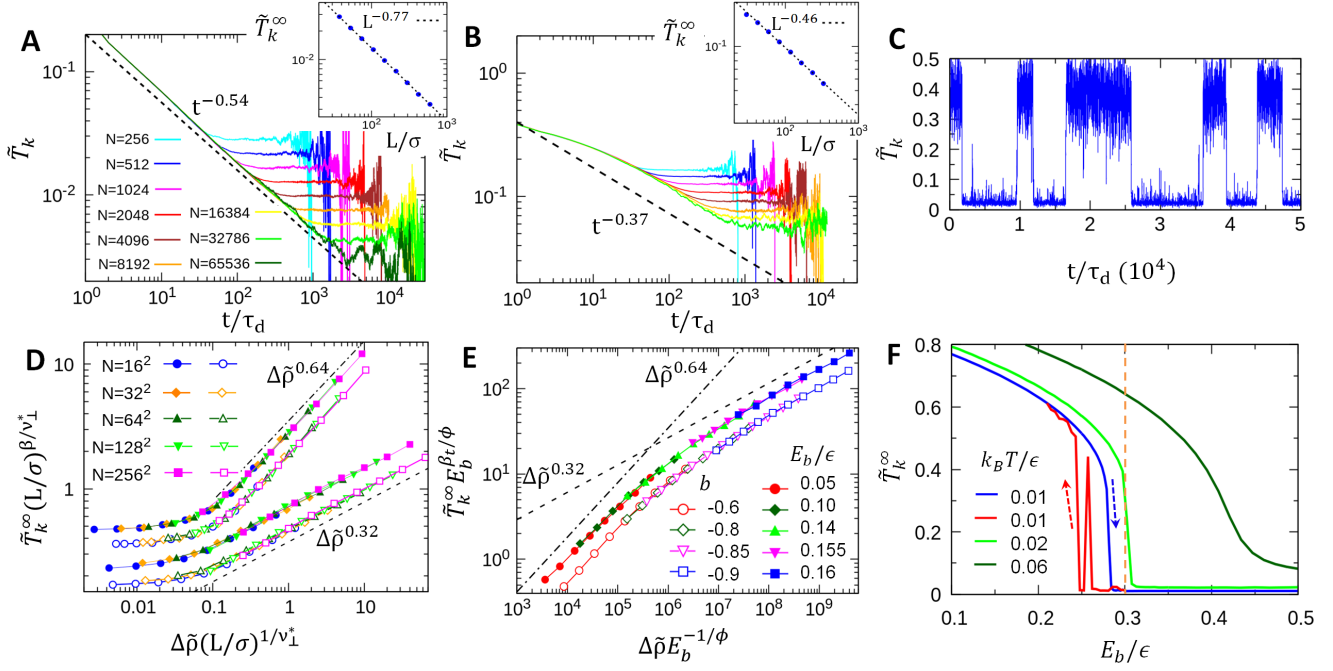


Fig. 2. Barrier-controlled criticality and discontinuous dynamic phase transition. (A and B) \tilde{T}_k as a function of time for different system sizes with inset showing saturated value as a function of system size. (A) $E_b = 0$, $\tilde{\rho} = 0.18471$; (B) $E_b = 0.165\epsilon$, $\tilde{\rho} = 0.29615$. (C) Demonstration of bistability at $E_b = 0.3\epsilon$, $\tilde{\rho} = 0.3290$ with thermal noise $k_B T = 0.02\epsilon$ for a system with $N = 1024$. (D) Collapse of $\tilde{T}_k(\Delta\tilde{\rho})$ according to Eq. (3) for different system sizes. Solid symbols are for reactive hard-sphere systems with $E_b = 0.0$ (upper), 0.165ϵ (lower), respectively. The open symbols are obtained in field simulations of Eq. (18-19) with $b = 1$ (upper), -0.92 (lower), respectively. (E) Crossover scaling analysis of the tricritical point based on Eq. (4). (F) \tilde{T}_k as a function of reaction barrier E_b at different thermal temperature T for 2D hard sphere systems at density $\tilde{\rho} = 0.3290$ and $N = 1024$. Hysteresis loop is found in system at $k_B T = 0.01\epsilon$ starting from different initial states as indicated by the dashed arrows. The yellow line indicates the density point at which the system exhibits clear bistability in C.

	$\beta(t)$	α	ν_{\perp}^*	z^*	ϕ
CDP	0.64(1)	0.52(1)	0.80(2)	1.53(2)	
$E_b = 0$	0.64(2)	0.54(2)	0.84(3)	1.50(3)	
$b = 1$	0.65(2)	0.53(2)	0.84(3)	1.51(2)	
$E_b = E_{b,c}$	0.32(4)	0.37(5)	0.68(4)	1.68(5)	0.32(5)
$b = b_c$	0.33(3)	0.36(4)	0.70(3)	1.65(5)	0.34(4)

Table 1. Critical exponents in 2D systems. Data for CDP is from (2, 51). Different values of E_b and b are for reactive hard-sphere model and field simulations of Eq. (18-19), respectively. Tricritical points are at $E_{b,c} = 0.165(5)\epsilon$ and $b_c = -0.92(3)$.

respectively. Here, f_a is the average activating collision frequency per particle which can be written as

$$f_a = x_a \bar{v}_a / (2l_r), \quad [6]$$

with x_a the fraction of activated particles and \bar{v}_a is the average speed of activated particles. l_r is the mean free path of activating collisions. At $E_b = 0$, l_r equals the mean free path of the system l_m since every collision induces an activation, while for $E_b > 0$, one can expect $l_r > l_m$ as discussed latter. Moreover, the driving power of thermal noise per particle W_{driv}^{therm} can be approximated by the equilibrium dissipation power $W_{disp}^{therm} = \gamma dk_B T / m$. Thus, the dynamic equation for

kinetic energy per particle can be written as

$$\begin{aligned} \epsilon \frac{\partial \tilde{T}_k}{\partial t} &= W_{driv} - W_{disp} + W_{driv}^{therm} \\ &= \frac{x_a \tilde{\rho}_r \bar{v}_a \epsilon}{2\sigma} - \gamma \bar{v}^2 + \frac{\gamma dk_B T}{m}. \end{aligned} \quad [7]$$

Here we use the low density approximation for the mean free path of activating collision $l_r \simeq \sigma / \tilde{\rho}_r$ with $\tilde{\rho}_r$ the density of effective reactant, i.e., the average density of particle that can be activated under \tilde{T}_k . For systems far from the critical point ($l_d \gg l_m$) the average kinetic energy would be much larger than the activation barrier ($\tilde{T}_k \gg E_b / \epsilon$), thus we have $\tilde{\rho}_r \simeq \tilde{\rho}$, $x_a \simeq 1$ and $\bar{v}_a \simeq \bar{v}$ with \bar{v} the average speed of all particles. Based on the approximation $\bar{v}^2 \simeq v^2 = dk_B T_k / m$, at zero thermal noise $T = 0$, the steady-state kinetic temperature \tilde{T}_k^∞ satisfying $\frac{\partial \tilde{T}_k}{\partial t} = 0$ can be obtained as (44)

$$\tilde{T}_k^\infty \simeq \frac{1}{4d} \left(\frac{l_d}{l_m} \right)^2, \quad [8]$$

which does not depend on E_b . This is verified in simulations as shown in the inset of Fig. 1. Nevertheless, for systems close to the critical point, there is strong dynamic heterogeneity, i.e., most particles are immobile and only a small fraction of particles are activated with typical excitation speed, i.e., $\bar{v}_a \simeq v_0$. Apparently, \bar{v}_a is a convex instead of concave function of x_a , since increasing x_a also increases the collision between activated particles, further raising \bar{v}_a . Thus, as a first-order approximation, we have

$$\bar{v}_a \simeq (1 + Ax_a)v_0 \quad [9]$$

$$\tilde{T}_k \simeq x_a m \bar{v}_a^2 / \epsilon \simeq x_a + 2Ax_a^2 \quad [10]$$

with the coefficient $A > 0$ indicating the convexness. Reversely, we can rewrite x_a as a function of order parameter \tilde{T}_k :

$$x_a \simeq \tilde{T}_k - 2A\tilde{T}_k^2. \quad [11]$$

Moreover, for systems with $E_b > 0$, one can expect that there would be a fraction of collisions between active and inactive particles that do not induce activation. This effect leads to the elongation of the mean free path of active collisions, or the decrease of the effective reactant density. Therefore, as a first-order approximation, we can have

$$\tilde{\rho}_r/\tilde{\rho} = 1 - B(1 - x_a)\tilde{E}_b \quad [12]$$

with the coefficient $B > 0$. Finally, by keeping only the first three leading terms, Eq. (7) can be written as

$$\frac{\partial \tilde{T}_k}{\partial \tilde{t}} = a\tilde{T}_k - b\tilde{T}_k^2 - c\tilde{T}_k^3 + h \quad [13]$$

with $\tilde{t} = t/\tau_0$ and

$$a = \frac{\tilde{\rho}}{2}(1 - B\tilde{E}_b) - \frac{\tau_0}{\tau_d} \quad [14]$$

$$b = -\frac{\tilde{\rho}}{2}[(1 + A)B\tilde{E}_b - A] \quad [15]$$

$$c = \frac{\tilde{\rho}}{2}[4A^2 + (3A - 4A^2)B\tilde{E}_b]. \quad [16]$$

$$h = \gamma\tau_0 dk_B T / (m\epsilon) \quad [17]$$

The solution of this cubic dynamic equation is given in Section B in *SI Appendix*. The corresponding phase diagram is summarized in Fig. 3. At zero thermal noise ($T = 0$) and $E_b < E_{b,c}$ (or $b > 0$), Eq.(13) has only one fixed point at $a = 0$ and the system undergoes a continuous phase transition with the mean-field critical exponent $\beta_{MF} = 1$ and upper critical dimension $d_c = 4$. The transition points are shown as an orange curve in Fig. 3. In contrast, when E_b increases above $E_{b,c}$ (or $b < 0$), Eq.(13) has two fixed points, which corresponds to a bistability or a discontinuous dynamic phase transition. Importantly, $E_b = E_{b,c}$ (or $b = 0$) is the tricritical point with $\beta_{MF} = 1/2$ and $d_c = 3$, which separates the continuous and discontinuous phase transitions (purple point in Fig. 3). In the presence of thermal noise ($T > 0$), the continuous phase transition is meshed out accompanied by the shrink of bistability region (enclosed by red and blue surfaces). This general picture is insensitive to the specific choice of coefficients A, B and agrees qualitatively with the simulation results.

Reggeon-field simulations. Next we go beyond the mean-field level by cooperating spatial-temporal fluctuations in the theory. In this scenario, the local temperature field $\tilde{T}_k^l(\mathbf{r}, t)$ is coupled with the local density field $\tilde{\rho}_l(\mathbf{r}, t)$, and the dynamic equations at arbitrary position \mathbf{r} satisfy,

$$\frac{\partial \tilde{T}_k^l}{\partial \tilde{t}} = a\tilde{T}_k^l - b\tilde{T}_k^{l2} - c\tilde{T}_k^{l3} + \lambda \nabla^2 \tilde{T}_k^l - h + \lambda \sqrt{\tilde{T}_k^l} \eta(\mathbf{r}, t) \quad [18]$$

$$\frac{\partial}{\partial \tilde{t}} \tilde{\rho}_l = D \nabla^2 \tilde{T}_k^l, \quad [19]$$

where, a, b , and c are functions of $\tilde{\rho}_l(\mathbf{r}, t)$ based on Eq. (14-16). The last term in Eq. (18) represents the spatial-temporal fluctuation with λ the noise magnitude. This fluctuation accounts for the chaos effects in the active state. The second dynamic equation (Eq. (19)) is the thermophoresis diffusion

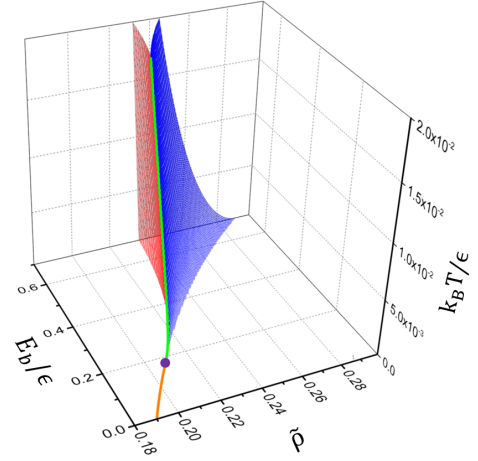


Fig. 3. Mean-field phase diagram. The orange line and green line represent of the CDP and Ising-type critical points of the system, respectively. The purple point is the tricritical point. The bistability region is enclosed by the blue and red surfaces. The parameters used is $A = 0.095$, $B = 1/2$ and $\tau_d/\tau_0 = 10$.

equation of the particles. Eq. (18-19), in fact, share the same formula as in the Reggeon-field theory of CDP (52). Since the criticality of dynamic equations does not depend on specific choice of parameters, the critical exponents for Eq. (18-19) should be the same as the standard Reggeon field theory in which b and $\tilde{\rho}$ are the controlling parameters with $a = a' \tilde{\rho}_l(\mathbf{r}, t) - a_0$. Other parameters are simply set as $a_0 = 1$, $a' = 1$, $c = 1$, $\lambda = 1$, $D = 1$, $h = 0$, $\Lambda = 1$ (52). Since the noise term is multiplicative, we adopt a numerical method based on Fokker-Planck equation (53) to integrate the standard Reggeon fields equations on square or cubic lattices. This method has been used to obtain the accurate critical exponents for both directed percolation and CDP (53), but not for the tricritical points. In Fig. 2D,E, the open symbols show the results from the field simulations, which behave essentially the same as the reactive hard-sphere system. The obtained (tri)critical exponents are also given in Table I, which are consistent with those from the hard-sphere systems. Moreover, the upper critical dimension $d_c = 3$ at tricriticality is also confirmed both in hard-sphere systems and field simulations (see Fig. S3-S6 and Table S1 in *SI Appendix*). This quantitative agreement further proves the validity of our theory and concludes that the universality of the reactive hard-sphere model at the edge of continuous absorbing phase transition belongs to the tricritical CDP universality.

Ising universality at finite thermal noise. Lastly, our theory predicts another critical line (the green line in Fig. 3) in the finite thermal temperature regime ($T > 0$), which satisfies $[a_c, b_c, \tilde{T}_{k,c}] = \left[-3 \left(\frac{h}{c} \right)^{2/3}, -3 \left(\frac{h}{c} \right)^{1/3}, \left(\frac{h}{c} \right)^{1/3} \right]$. The universality class of similar noise-induced critical points has been under debate for a long time, first initiated by the Schoggl's second model (54-59), later extended into dynamic network models (60-62). In the following, we provide a new theoretical argument which suggests that this critical line belongs to the Ising universality. The core of this argument is that around the critical point $[a_c, b_c]$, we can find a direction in the (a, b) parameter space, i.e., $(\tilde{T}_{k,c}, 1)$, along which Eq.(13) can be

rewritten as

$$\frac{\partial \Delta \tilde{T}_k}{\partial \tilde{t}} \simeq -c \Delta \tilde{T}_k (\Delta \tilde{T}_k^2 + \tilde{T}_{k,c} \Delta b / c), \quad [20]$$

with $\Delta \tilde{T}_k = \tilde{T}_k - \tilde{T}_{k,c}$ and $\Delta b = b - b_c$ (see Method section). Therefore, for $\Delta b < 0$, the system has two stable fix points $\Delta \tilde{T}_k \simeq \pm \sqrt{-\Delta b \tilde{T}_{k,c} / c}$, which indicates $\beta_{MF} = 1/2$, consistent with the Ising universality. More importantly, Eq. (20) has \mathbb{Z}_2 symmetry under the transformation ($\Delta \tilde{T}_k \rightarrow -\Delta \tilde{T}_k$), another evidence for the Ising universality. It should be noted that our conclusion is different from a recent theoretical work of a dynamic network model (61, 62), in which the authors only did the perturbation along the orthogonal directions (1, 0) and (0, 1) and obtained an incorrect $\beta_{MF} = 1/3$. Accordingly, the authors concluded a DP-type universality for this transition. In fact, systems described by the above cubic equations can be mapped to the ϕ^4 Landau-Ginzburg theory, and generically belong to the Ising universality class with nonconservative (model A) dynamics (14, 55, 63).

Conclusion and Discussion

In conclusion, by using simulation and theoretical analysis, we systematically investigate the criticality of a reactive hard sphere model with an activation barrier. We find that increasing the activation barrier effectively delays the dynamic transition but also increases the transition cooperativity which sharpens the transition. The cooperativity gain raised by the activation barrier is different from that in the Schlogl's second model (3), where the cooperativity is enforced by a topological property, i.e., the number of active neighbours. It is also different from the explosive percolation model which relies on information input to avoid the occurrence of the larger cluster (47, 64, 65). In fact, the cooperativity comes from the inertia of particles, which makes it possible for previous activation to facilitate the consecutive ones. A similar memory-induced cooperativity has also been reported in a contagion network model system (66). Our finding have a direct implication for exothermic chemical reactions, where it was suggested that increasing the activation energy can make the reactions change from slow combustion to thermal explosion (67, 68). Similar mechanism of barrier-controlled criticality should also exist in nuclear chain reactions, which is highly relevant with the nuclear criticality safety (69). Moreover, this could be also related with the criticality of dynamic phase transition in random organization systems. For examples, it was found in experiments that for high density colloidal suspensions under oscillatory shearing, the geometrical protection from neighbouring particles suppresses or cancels the activated displacement, which sharpens the transition (26). Similar discontinuous dynamic phase transitions have also been observed in driven amorphous solids (28, 33), the glass transition systems (70) and high-density active matter systems (43, 71). In all these cases, particles need to cross energy barriers or cages set by their neighbors to be activated. Although the activation in these systems is different from our model, they share the same ideas of delay sharpening the phase transition. Therefore, it is plausible that near the critical point they are governed by the same cubic dynamic equation. Additionally, the activation barrier investigated in our work can be also seen as the virus load threshold for contagious diseases or the signal magnitude threshold for information transmission. Therefore, our finding

about the activation barrier on the criticality of a minimal reactive hard sphere model, can not only help understand the criticality of reactive particle systems, e.g., chemical reactions, but also shed lights in the dynamic behaviour of amorphous materials and active matter, as well as the spread of epidemic, knowledge and innovations (5).

Materials and Methods

Finite-size analysis to obtain dynamic exponent z and the solution of cubic dynamic equation can be found in *SI Appendix*.

ACKNOWLEDGMENTS. This work has been supported in part by the Singapore Ministry of Education through the Academic Research Fund MOE2019-T2-2-010 and RG104/17 (S), by Nanyang Technological University Start-Up Grant (NTU-SUG: M4081781.120), by the Advanced Manufacturing and Engineering Young Individual Research Grant (A1784C0018) and by the Science and Engineering Research Council of Agency for Science, Technology and Research Singapore. We thank NSCC for granting computational resources.

- Hinrichsen H (2000) Non-equilibrium critical phenomena and phase transitions into absorbing states. *Advances in physics* 49(7):815–958.
- Henkel M, Hinrichsen H, Lübeck S (2008) *Non-equilibrium phase transitions: Absorbing Phase Transitions*. (Springer) Vol. 1.
- Schlögl F (1972) Chemical reaction models for non-equilibrium phase transitions. *Zeitschrift für physik* 253(2):147–161.
- Claycomb J, Bassler K, Miller Jr J, Nersisyan M, Luss D (2001) Avalanche behavior in the dynamics of chemical reactions. *Phys. Rev. Lett.* 87(17):178303.
- Pastor-Satorras R, Castellano C, Van Mieghem P, Vespignani A (2015) Epidemic processes in complex networks. *Rev. Mod. Phys.* 87(3):925.
- Munoz MA (2018) Colloquium: Criticality and dynamical scaling in living systems. *Rev. Mod. Phys.* 90(3):031001.
- Pine DJ, Gollub JP, Brady JF, Leshansky AM (2005) Chaos and threshold for irreversibility in sheared suspensions. *Nature* 438(7070):997–1000.
- Corte L, Chaikin P, Gollub JP, Pine D (2008) Random organization in periodically driven systems. *Nat. Phys.* 4(5):420–424.
- Regev I, Weber J, Reichhardt C, Dahmen KA, Lookman T (2015) Reversibility and criticality in amorphous solids. *Nat. Commun.* 6:8805.
- Bak P, Tang C, Wiesenfeld K (1987) Self-organized criticality: An explanation of the 1/f noise. *Phys. Rev. Lett.* 59(4):381.
- Takeuchi KA, Kuroda M, Chaté H, Sano M (2007) Directed percolation criticality in turbulent liquid crystals. *Physical review letters* 99(23):234503.
- Schaller V, Weber CA, Hammerich B, Frey E, Bausch AR (2011) Frozen steady states in active systems. *Proc. Natl. Acad. Sci. U.S.A* 108(48):19183–19188.
- Shi Xq, Ma Yq (2013) Topological structure dynamics revealing collective evolution in active nematics. *Nat. Commun.* 4:3013.
- Partridge B, Lee CF (2019) Critical motility-induced phase separation belongs to the ising universality class. *Phys. Rev. Lett.* 123(6):068002.
- Harris TE (1974) Contact interactions on a lattice. *The Annals of Probability* pp. 969–988.
- Manna S (1991) Two-state model of self-organized criticality. *J. Phys. A: Math. Gen.* 24(7):L363.
- Rossi M, Pastor-Satorras R, Vespignani A (2000) Universality class of absorbing phase transitions with a conserved field. *Phys. Rev. Lett.* 85(9):1803.
- Chou DP, Yip S (1982) Computer molecular dynamics simulation of thermal ignition in a self-heating slab. *Combustion and Flame* 47:215–218.
- Chou DP, Yip S (1984) Molecular dynamics simulation of thermal ignition in a reacting hard sphere fluid. *Combustion and flame* 58(3):239–253.
- Baras F, Mansour MM (1989) Validity of macroscopic rate equations in exothermic chemical systems. *Phys. Rev. Lett.* 63(21):2429.
- Nowakowski B, Lemarchand A (2001) Stochastic effects in a thermochemical system with newtonian heat exchange. *Phys. Rev. E* 64(6):061108.
- Semenov N (1928) Theories of combustion process. *Z. Phys. Chem.* 48:571–582.
- Semenov N (1959) *Some Problems of Chemical Kinetics and Reactivity*. Vol. 1 & 2.
- Corte L, Gerbode S, Man W, Pine D (2009) Self-organized criticality in sheared suspensions. *Phys. Rev. Lett.* 103:248301.
- Franceschini A, Filippini E, Guazzelli E, Pine DJ (2011) Transverse alignment of fibers in a periodically sheared suspension: an absorbing phase transition with a slowly varying control parameter. *Phys. Rev. Lett.* 107(25):250603.
- Jeanneret R, Bartolo D (2014) Geometrically protected reversibility in hydrodynamic loschmidt-echo experiments. *Nat. Commun.* 5(1):1–8.
- Leishangthem P, Parmar AD, Sastry S (2017) The yielding transition in amorphous solids under oscillatory shear deformation. *Nature communications* 8(1):1–8.
- Das P, Vinutha H, Sastry S (2020) Unified phase diagram of reversible–irreversible, jamming, and yielding transitions in cyclically sheared soft-sphere packings. *Proceedings of the National Academy of Sciences* 117(19):10203–10209.
- Ness C, Cates ME (2020) Absorbing-state transitions in granular materials close to jamming. *Physical Review Letters* 124(8):088004.

30. Ness C, Mari R, Cates ME (2018) Shaken and stirred: Random organization reduces viscosity and dissipation in granular suspensions. *Science advances* 4(3):eaar3296.
31. Milz L, Schmiedeberg M (2013) Connecting the random organization transition and jamming within a unifying model system. *Phys. Rev. E* 88(6):062308.
32. Zhou C, Reichhardt CO, Reichhardt C, Beyerlein I (2014) Random organization in periodically driven gliding dislocations. *Physics Letters A* 378(22-23):1675–1678.
33. Nagasawa K, Miyazaki K, Kawasaki T (2019) Classification of the reversible–irreversible transitions in particle trajectories across the jamming transition point. *Soft matter* 15(38):7557–7566.
34. Royer JR, Chaikin PM (2015) Precisely cyclic sand: Self-organization of periodically sheared frictional grains. *Proc. Natl. Acad. Sci. U.S.A* 112(1):49–53.
35. Mangan N, Reichhardt C, Reichhardt CO (2008) Reversible to irreversible flow transition in periodically driven vortices. *Phys. Rev. Lett.* 100(18):187002.
36. Reichhardt C, Reichhardt CO (2009) Random organization and plastic depinning. *Phys. Rev. Lett.* 103(16):168301.
37. Okuma S, Tsugawa Y, Motohashi A (2011) Transition from reversible to irreversible flow: Absorbing and depinning transitions in a sheared-vortex system. *Phys. Rev. B* 83(1):012503.
38. Hexner D, Levine D (2015) Hyperuniformity of critical absorbing states. *Phys. Rev. Lett.* 114(11):110602.
39. Tjhung E, Berthier L (2015) Hyperuniform density fluctuations and diverging dynamic correlations in periodically driven colloidal suspensions. *Phys. Rev. Lett.* 114(14):148301.
40. Weijs JH, Jeanneret R, Dreyfus R, Bartolo D (2015) Emergent hyperuniformity in periodically driven emulsions. *Phys Rev Lett* 115(10):108301.
41. Hexner D, Levine D (2017) Noise, diffusion, and hyperuniformity. *Phys. Rev. Lett.* 118(2):020601.
42. Wang J, Schwarz JM, Paulsen JD (2018) Hyperuniformity with no fine tuning in sheared sedimenting suspensions. *Nat. Commun.* 9(1):2836.
43. Lei QL, Ciamarra MP, Ni R (2019) Nonequilibrium strongly hyperuniform fluids of circle active particles with large local density fluctuations. *Sci. Adv.* 5(1):eaau7423.
44. Lei QL, Ni R (2019) Hydrodynamics of random-organizing hyperuniform fluids. *Proc. Natl. Acad. Sci. U.S.A* 116(46):22983–22989.
45. Ma Z, Torquato S (2019) Hyperuniformity of generalized random organization models. *Physical Review E* 99(2):022115.
46. Scala A (2012) Event-driven langevin simulations of hard spheres. *Phys. Rev. E* 86(2):026709.
47. Achlioptas D, D'Souza RM, Spencer J (2009) Explosive percolation in random networks. *Science* 323(5920):1453–1455.
48. Lübeck S (2006) Tricritical directed percolation. *J Stat Phys* 123(1):193–221.
49. Janssen HK, Müller M, Stenull O (2004) Generalized epidemic process and tricritical dynamic percolation. *Phys. Rev. E* 70(2):026114.
50. Araújo NA, Andrade Jr JS, Ziff RM, Herrmann HJ (2011) Tricritical point in explosive percolation. *Phys. Rev. Lett.* 106(9):095703.
51. Lee SB (2013) Comment on “fixed-energy sandpiles belong generically to directed percolation”. *Phys. Rev. Lett.* 110(15):159601.
52. di Santo S, Burioni R, Vezzani A, Muñoz MA (2016) Self-organized bistability associated with first-order phase transitions. *Phys. Rev. Lett.* 116(24):240601.
53. Dornic I, Chaté H, Munoz MA (2005) Integration of langevin equations with multiplicative noise and the viability of field theories for absorbing phase transitions. *Phys. Rev. Lett.* 94(10):100601.
54. Dewel G, Walgraef D, Borckmans P (1977) Renormalization group approach to chemical instabilities. *Zeitschrift für Physik B Condensed Matter* 28(3):235–237.
55. Brachet M, Tirapegui E (1981) On the critical behaviour of the schlögl model. *Phys. Lett. A* 81(4):211–214.
56. Dewel G, Borckmans P, Walgraef D (1981) Nonequilibrium phase transitions and chemical instabilities. *J. Stat. Phys.* 24(1):119–137.
57. Grassberger P (1981) On phase transitions in schlögl's second model in *Nonlinear Phenomena in Chemical Dynamics*. (Springer), pp. 262–262.
58. Tomé T, Dickman R (1993) Ziff-gulari-barshad model with co desorption: An ising-like nonequilibrium critical point. *Phys. Rev. E* 47(2):948.
59. Liu DJ, Pavlenko N, Evans JW (2004) Crossover between mean-field and ising critical behavior in a lattice-gas reaction-diffusion model. *J. Stat. Phys.* 114(1-2):101–114.
60. Majdandzic A, et al. (2014) Spontaneous recovery in dynamical networks. *Nat. Phys.* 10(1):34–38.
61. Böttcher L, Nagler J, Herrmann HJ (2017) Critical behaviors in contagion dynamics. *Phys. Rev. Lett.* 118(8):088301.
62. Böttcher L, Luković M, Nagler J, Havlin S, Herrmann HJ (2017) Failure and recovery in dynamical networks. *Sci. Rep.* 7(1):1–9.
63. Hohenberg PC, Halperin BI (1977) Theory of dynamic critical phenomena. *Rev. Mod. Phys.* 49(3):435.
64. Cho YS, Hwang S, Herrmann HJ, Kahng B (2013) Avoiding a spanning cluster in percolation models. *Science* 339(6124):1185–1187.
65. D'Souza RM, Nagler J (2015) Anomalous critical and supercritical phenomena in explosive percolation. *Nat. Phys.* 11(7):531–538.
66. Dodds PS, Watts DJ (2004) Universal behavior in a generalized model of contagion. *Phys. Rev. Lett.* 92(21):218701.
67. Boddington T, Gray P, Robinson C (1979) Thermal explosions and the disappearance of criticality at small activation energies: exact results for the slab. *Proceedings of the Royal Society of London. A. Mathematical and Physical Sciences* 368(1735):441–461.
68. Lacey A (1983) Critical behaviour of homogeneous reacting systems with large activation energy. *Int. J. Eng. Sci.* 21(5):501–515.
69. Lamarsh JR, Baratta AJ (2001) *Introduction to nuclear engineering*. (Prentice hall Upper Saddle River, NJ) Vol. 3.
70. Hedges LO, Jack RL, Garrahan JP, Chandler D (2009) Dynamic order-disorder in atomistic models of structural glass formers. *Science* 323(5919):1309–1313.
71. Tjhung E, Berthier L (2017) Discontinuous fluidization transition in time-correlated assemblies of actively deforming particles. *Phys. Rev. E* 96(5):050601.